Research

Authors for correspondence:
Peng Song
e-mail: songpengkm@163.com
Jing Feng
e-mail: jingfeng@kmust.edu.cn

Fabrication and characterization of Ni-decorated h-BN powders with ChCl-EG ionic liquid as addition by electroless deposition

Qionglian Yang[1], Juanjian Ru[2], Peng Song[1], Mingyu Hu[1] and Jing Feng[1]

[1]Faculty of Materials Science and Engineering, and [2]Faculty of Metallurgical and Energy Engineering, Kunming University of Science and Technology, Kunming 650093, People's Republic of China

(iD) QY, 0000-0001-5384-976X

Ni-decorated h-BN powders are fabricated with ChCl-EG as additive via electroless plating in the paper. As comparison, the different additive concentration of choline chloride-ethylene glycol (ChCl-EG) ionic liquid ($0\,g\,l^{-1}$, $30\,g\,l^{-1}$, $60\,g\,l^{-1}$, $90\,g\,l^{-1}$) is presented. The effects of ChCl-EG concentration are studied, including the surface morphologies, phase analysis of Ni-decorated h-BN powders and the residual Ni^{2+} concentration is measured in electroless plating bath. It is demonstrated that the deposition phenomena of nickel particles on h-BN surface is changed with the addition of ChCl-EG. When the concentration of ChCl-EG is $30\,g\,l^{-1}$, the Ni particles on h-BN surface are in dispersed and spheroid state with the average size of 10–1000 nm. It can be found that $30\,g\,l^{-1}$ ChCl-EG is conducive to the arise of deposition phenomena, which is the formation of the single nickel particle on h-BN surface. Besides, more Ni particles are deposited on h-BN surface with the increase of nickel plating times, which is characterized with scanning electron microscope and transmission electron microscope. Furthermore, the deposition phenomenon and growth mechanism are proposed without and with ChCl-EG as additive to further elaborate the formation of Ni particles on h-BN surface.

THE ROYAL SOCIETY
PUBLISHING

1. Introduction

Electroless deposition process is an autocatalytic chemical reaction in aqueous solution which is used in surface metallization of conductive or non-conductive substrates, the extensive and potential surface engineering has been much faster developed [1–4]. The potential technique can be related to its unique quality of surface modification, such as the hardness, wettability, corrosion properties and the capability to generate distributed deposition on different materials [5–7]. Comparing with the conventional electroplating process, the electroless deposition technique offers impressive advantages in terms of lower processing cost because the electricity is not involved. It is possible for getting deposition on materials with the excellent properties by adjusting of the composition, the pH and the temperature of an electroless bath [8–10]. Over the years, the various micro and nano hard particles (SiC, TiC, WC, Cr_3C_2, Al_2O_3, etc.) have been successfully coprecipitated by the electroless deposition process to surface modification [6,11–19]. Otherwise, molybdenum disulfide [20–23], polytetrafluoroethylene [24–26], graphite [10,11,27] and carbon nanotubes [28,29] as soft lubricating particles have been developed to get self-lubricating electroless composite materials. Hexagonal boron nitride (h-BN) is another excellent high-temperature solid lubricant with the layered structure analogous to MoS_2 and graphite [10,26], the solid lubricant is a promising alternative candidate material in special environment [30–32]. Nevertheless, some relevant reports reveal that h-BN has been relatively the least explored in tribology owing to its poor wettability with ceramic/metal matrix and its inadequate thermo-oxidative performance [5,31,33]. Li *et al*. revealed the incorporation of h-BN lubricant powders within matrix layer of active metal, as nickel could be used to improve the wettability performance of h-BN, and they had shown the optimal process of nickel-coated boron nitride [34–36]. Zhao *et al*. employed the hydrothermal hydrogen reduction to fabricate nickel-coated hexagonal BN particles [35,36]. Besides, Du *et al*. indicated the use of Ni-coated h-BN for laser treated composite coating [5,30]. Thus, detailed insights of depositing nickel particles on h-BN surface via the electroless deposition become an interesting problem.

Electroless deposition process has been explored in order to deposit nickel particles on h-BN surface. However, the instability of electroless plating bath limits the application of the process, because the Ni ions cannot be effectively used and they are easy to be deposited with the cluster in the electroless bath [16,37]. To overcome these shortcomings, a new kind of plating solution or additive needs to be found for the process. Recently, there has been a growing interest of the new class of substance with low melting point and vapour pressure, good conductivity, non-flammability and wide electrochemical window, named as room temperature ionic liquids [38]. Up to now, lots of studies have been reported on the application of ionic liquid as additives, such as lubricant additives [39,40], catalytic reactions and organics, and mobile-phase additives in liquid chromatography [41,42]. The research indicated that the addition of ionic liquids can effectively relieve the harmful effects of depositing quality and impurities. Therefore, Ru *et al*. fabricated Ni-decorated Al_2O_3 powders with [bmim] ionic liquid as additive, decreasing Ni clusters on the surface of Al_2O_3 powders and electroless plating bath. It is optimized that Ni particles are absolutely and uniformly deposited on the surface of powders [2,5,6].

In this paper, Ni-decorated h-BN powders are fabricated by electroless deposition from sulfate solution with ChCl-EG ionic liquid as additive. The effects of ChCl-EG concentration are studied, including the surface morphologies, the residual Ni^{2+} concentration is measured in electroless plating bath and the element distribution of Ni-decorated h-BN powders. Besides, the morphologies of coated products obtained with different nickel plating times are investigated. Based on the experimental results, an empirical model of deposition phenomenon without and with ChCl-EG as additive is proposed to further elaborate the formation mechanism of Ni-decorated h-BN powders.

2. Material and methods

2.1. Chemicals

All the chemicals used in this work were purchased commercially with analytical grade (purity > 99.90%) from Chemical Reagent Co., Shanghai, China. Micrometre-sized flaky h-BN powder with a mean particle size of about 1–30 μm and the crystal structure of h-BN particle were supplied, as illustrated in figure 1.

2.2. Synthesis of ChCl-EG ionic liquid

ChCl-EG ionic liquid was used as the additive in the electroless deposition of Ni-decorated h-BN powders. ChCl-EG ionic liquid was synthesized from choline chloride (ChCl) and ethylene glycol (EG)
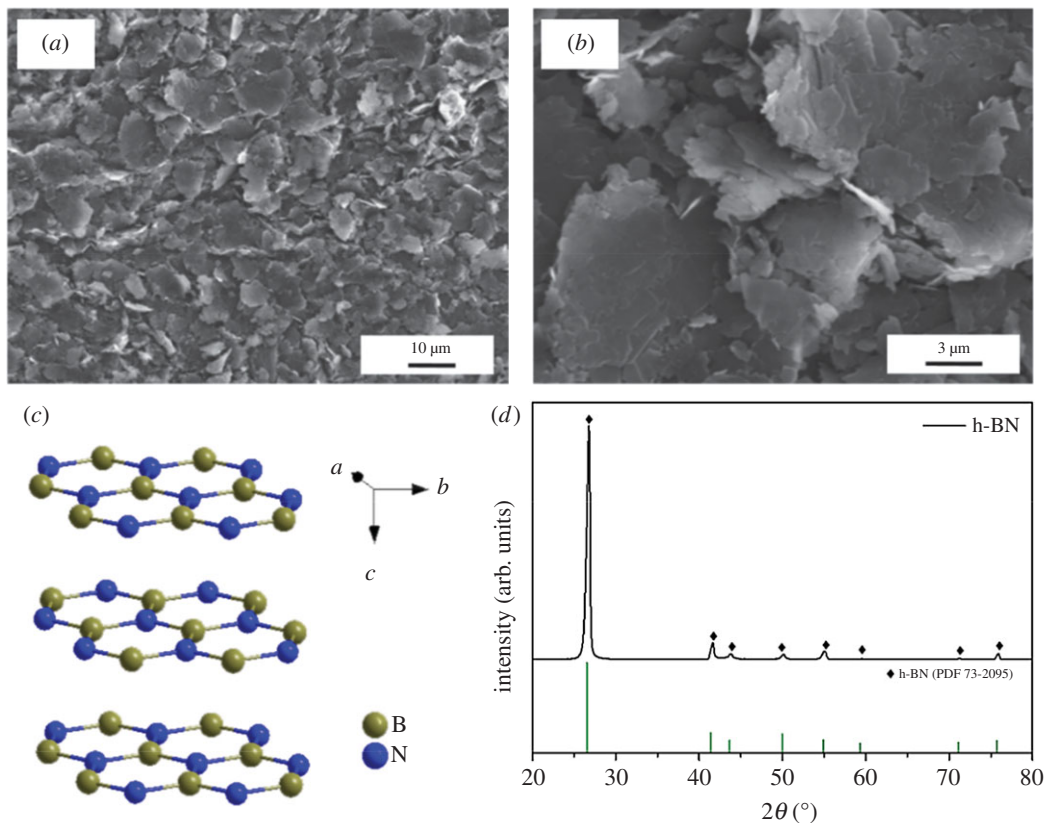
Figure 1. (*a,b*) SEM micrograph, (*c*) crystal structure and (*d*) XRD pattern of h-BN powders.

under a dry vacuum atmosphere [2,9,43], and then re-crystallized to form a new deep eutectic solution (DES). The ChCl-EG DES was fabricated by mixing ChCl and EG (the molar ratio was 1 : 2) together and stirring the mixed components at 353 K until a homogeneous, colourless liquid formed. The eutectic melt was dried under vacuum for 24 h at a temperature of 333 K and stored in a capped glass bottle.

2.3. Pretreatment of h-BN

The Ni-decorated h-BN powders were fabricated by pretreatment process and electroless deposition. At first, h-BN powders were washed in the mixing solution of acetone and ethanol (the molar ratio 1 : 2) with the ultrasound for 15 min to remove the surface impurities. Then, the h-BN powders were repeatedly washed with distilled water to neutral and obtained by precipitation and dried in a vacuum oven at 353 K [5,29].

2.4. Fabrication of Ni-decorated h-BN powders

The electroless deposition of Ni particles on h-BN surface was performed in an electroless solution with Ni^{2+}. The composition and concentration of the materials used in the electroless nickel bath are presented in table 1. First, 25 g $NiSO_4 \cdot 6H_2O$ was dissolved with 100 ml deionized water under the mechanical stirring speed of 300 r.p.m. Similarly, 16.5 g $NaH_2PO_2 \cdot H_2O$ and 20 g $C_6H_5Na_3O_7 \cdot 2H_2O$ can also be, respectively, dissolved with 100 ml deionized water under 300 r.p.m.; 12.5 g H_3BO_3 was dissolved with 200 ml deionized water under 300 r.p.m. and 40°C. Then, $NaH_2PO_2 \cdot H_2O$ solution, $C_6H_5Na_3O_7 \cdot 2H_2O$ solution and H_3BO_3 solution was added into $NiSO_4 \cdot 6H_2O$ solution in turn under 500 r.p.m. A small amount of NaOH solution was added into the above mixture solution to adjust pH of 8–9. Thus, the electroless plating bath was obtained according to above steps; 5 g h-BN was added into the above 500 ml electroless plating bath. Following that ChCl-EG ($0 \, g \, l^{-1}$, $30 \, g \, l^{-1}$, $60 \, g \, l^{-1}$, $90 \, g \, l^{-1}$) as additive were studied in the paper [5]. Besides, different nickel plating times (one time, three times, five times) were selected to investigate the deposition phenomenon of Ni particles on h-BN surface. All reactions were carried out with a mechanical stirring speed of 300 r.p.m. min^{-1} and 60°C. The Ni-decorated h-BN

Table 1. Chemical composition of the electroless plating bath and operating parameters.

role in bath or operating parameters	constituent	concentration or conditions
main salt	nickel sulfate ($NiSO_4 \cdot 6H_2O$)	50 g l^{-1}
reducing agent	sodium hypophosphite ($NaH_2PO_2 \cdot H_2O$)	33 g l^{-1}
complexing agent	tri-sodium citrate ($C_6H_5Na_3O_7 \cdot 2H_2O$)	40 g l^{-1}
buffering agent	boric acid (H_3BO_3)	25 g l^{-1}
pH adjuster	sodium hydroxide (NaOH)	to adjust pH
h-BN powder	—	10 g l^{-1}
mechanical stirring	—	300 r.p.m.
temperature	—	333 K
additive	ionic liquid (ChCl-EG)	0–90 g l^{-1}
pH	—	8–9

powders were characterized after washing with distilled water several times, filtrated and dried in a vacuum oven at 353 K for 6 h. The electroless deposition experiments were repeated three times to ensure the reproducibility.

2.5. Measurements and characterization

The surface morphology and elemental compositions of Ni-decorated h-BN powders were characterized by scanning electron microscope (SEM: ZEISS EVO 18) equipped energy dispersive spectroscopy (EDS: Bruker Quantax 200). Besides, the microstructures and crystallinity of sample were investigated by high-resolution transmission electron microscope (HRTEM: JEOL JEM-2100F). The utilization of nickel ions in electroless plating bath was measured via the inductively coupled plasma optical emission spectrometer (ICPOES: Optima 8000). The phases of the products were analysed by XRD (Rigaku MiniFlex 600) with Cu K$_\alpha$-radiation at a scan rate of 10° min^{-1} in the range of $2\theta = 20$–80°.

3. Results and discussion

3.1. Effects of ChCl-EG additive on Ni-decorated h-BN powders

In order to analyse the effect of ChCl-EG ionic liquid on the electroless deposition technique, the deposition experiments with different concentration of ChCl-EG are performed. Figure 2*a* is the residual Ni^{2+} concentration in electroless plating bath after different reaction time corresponding to the ChCl-EG concentration by the ICPOES analysis. It shows that the Ni^{2+} concentration in electroless plating bath is minimum with 30 g l^{-1} ChCl-EG as additive at any reaction time, this indicates that 30 g l^{-1} ChCl-EG ionic liquid is beneficial to deposit Ni particles from the solution. Besides, the XRD patterns of Ni-decorated h-BN powders fabricated with 0 g l^{-1}, 30 g l^{-1}, 60 g l^{-1}, 90 g l^{-1} ChCl-EG as additive are indicated in figure 2*b*. It can be found that with the ChCl-EG concentration of 30 g l^{-1}, the main phases of the samples are h-BN and metallic Ni, whereas the phosphorus is not observed, which may be below 4–5% and not characterized by XRD. The diffraction patterns of h-BN are in accordance with JCPDS card 73-2095 and that of Ni corresponds to JCPDS card 87-0712. The above results indicate that metallic Ni can be deposited from sulfate solution successfully when ChCl-EG ionic liquid is used as additive. Remarkably, the characteristic peaks of h-BN powders are distinct and sharp, but that of metallic Ni are weaker and broader with preferred orientation (111) plane, which can be ascribed to the poor crystallinity of metallic Ni. Besides, the XRD pattern of Ni-decorated h-BN powders obtained with 30 g l^{-1} ChCl-EG as additive is almost analogous to that of powders fabricated without ChCl-EG. However, the diffraction peaks of metallic Ni are much weaker when the addition of ChCl-EG is 60 g l^{-1} and 90 g l^{-1}. It demonstrates the deposition of Ni grains cannot be affected with 30 g l^{-1} ChCl-EG as additive, conversely, it can be promoted in the reaction process, and this will be discussed in the following.
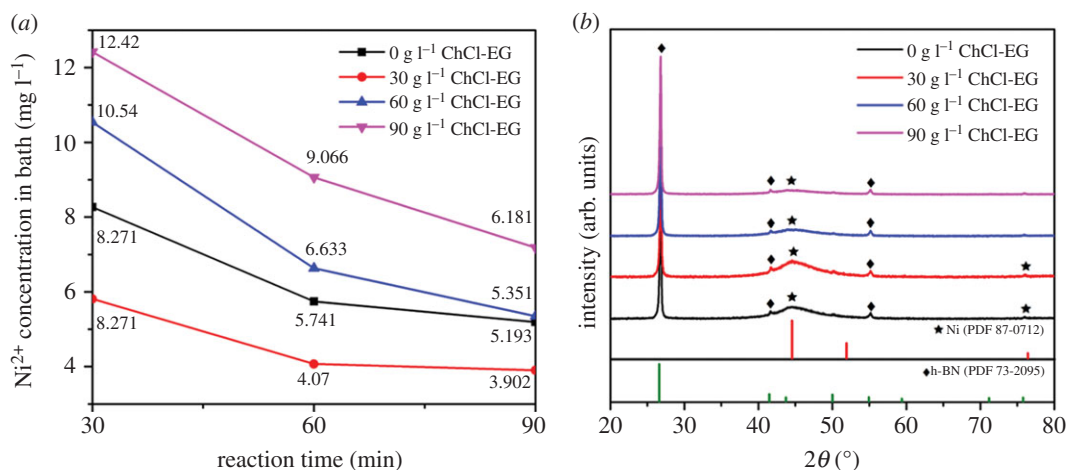
Figure 2. (*a*) The Ni^{2+} concentration in electroless solution in different reaction time, (*b*) XRD patterns of Ni-decorated h-BN powders fabricated with 0 g l^{-1}, 30 g l^{-1}, 60 g l^{-1} and 90 g l^{-1} ChCl-EG as additive.
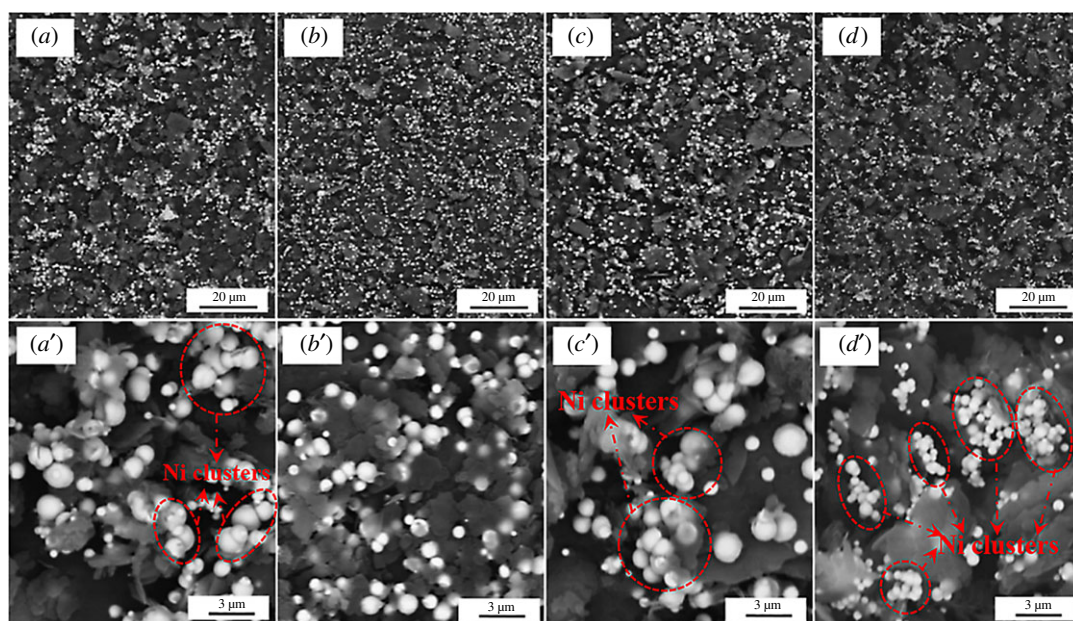

Figure 3. SEM morphologies of Ni-decorated h-BN powders in different concentration of ChCl-EG as additive (*a,a′*) 0 g l^{-1}, (*b,b′*) 30 g l^{-1}, (*c,c′*) 60 g l^{-1} and (*d,d′*) 90 g l^{-1}.

The surface morphologies of Ni-decorated h-BN powders fabricated with different concentration of ChCl-EG are shown in figure 3*a–d′*. From figure 3*a,a′*, without ChCl-EG adding, there are many Ni clusters on the surface of h-BN, which are marked by the red dotted line, and the Ni particles are the uneven size. In addition, much Ni-free h-BN surface could be observed and small amounts of the independent Ni particles are scattered on h-BN powders. Those Ni particles are also spheroidal with a size of about 100–1500 nm. Accordingly, figure 4*a$_0$–a$_4$* shows the element distribution of Ni-decorated h-BN powders fabricated without ChCl-EG as additive. There is also a strong Ni peak in the EDS spectrum. The element content of Ni and P are 10.01 at.% and 1.12 at.%, respectively. The content of Ni is slight lower than that of product obtained with 30 g l^{-1} ChCl-EG as additive while that of P is much the same. However, it can be seen that the many Ni clusters deposited on the surface of h-BN powders and most Ni particles with the uneven size are found from figure 3*a,a′* and figure 4*a*.

When the ChCl-EG concentration is 30 g l^{-1}, the Ni grains are deposited on the surface of flake h-BN powders and there hardly have the agglomerated Ni powders formed (figure 3*b,b′*), as mentioned in
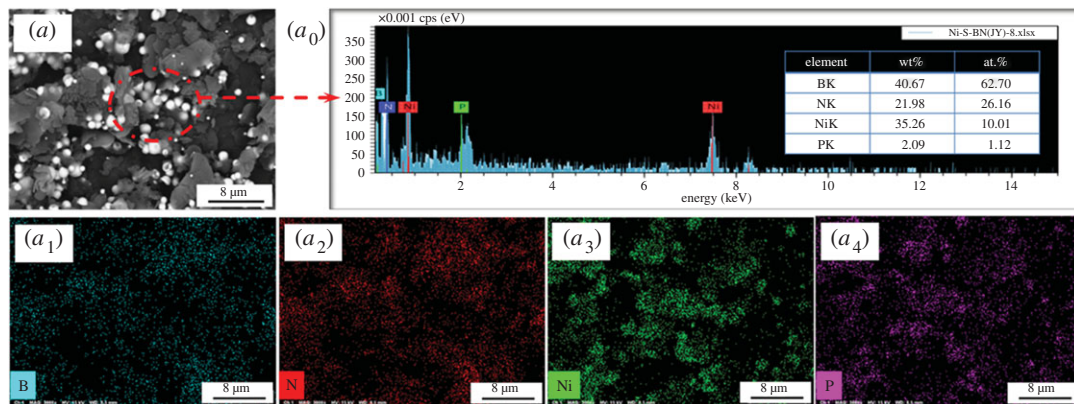
Figure 4. SEM morphologies (*a*) and EDS analysis (*a*$_0$–*a*$_4$) of Ni-decorated h-BN powders without ChCl-EG as additive.

§3.2. With increase of ChCl-EG concentration to $60\,g\,l^{-1}$, the Ni particles are distributed on the surface of h-BN, as is shown in figure 3*c*–*c'*, and the distribution is among the samples without ChCl-EG and with $30\,g\,l^{-1}$ ChCl-EG as additive. Besides, a part of Ni clusters come into being and the size of Ni particles is inhomogeneous on h-BN powders with a size distribution of 50–2000 nm. At a higher ChCl-EG concentration of $90\,g\,l^{-1}$ (figure 3*d,d'*), it is obviously seen that there are a lot of Ni clusters on h-BN powders and the size of Ni particles are much smaller, about 10–700 nm, which is nearly one-third as large as that of Ni particles in figure 3*c'*. Besides, the content of Ni is much less than the above three samples ($0\,g\,l^{-1}$, $30\,g\,l^{-1}$, $60\,g\,l^{-1}$ ChCl-EG as additive). Therefore, the metallic Ni in those samples detected is consistent with XRD examination (figure 2*b*). Based on the above comparative analysis, addition of $30\,g\,l^{-1}$ ChCl-EG ionic liquid is optimum to obtain the Ni-decorated h-BN powders without Ni clusters on h-BN powders via electroless deposition.

3.2. Fabrication of Ni-decorated h-BN powders with 30 g l^{-1} ChCl-EG as optimum additive

The SEM micrograph analysis of Ni-decorated h-BN powders fabricated with $30\,g\,l^{-1}$ ChCl-EG as additive are illustrated in figure 5*a*–*c*. From figure 5*a*, the bright white Ni particles are deposited on the surface of flake h-BN powders and part of the h-BN surface is decorated by spheroidal Ni particles. A small amount of Ni clusters can be deposited on the surface of h-BN powders, and most Ni particles are in the dispersed state. As shown in figure 5*b*, the Ni particles are independently distributed on the surface of loosely accumulated flake h-BN powders. In addition, these little Ni particles are globular, with a mean size of about 10–1000 nm, and it can be also deposited on the region between layers, besides the surface of h-BN powders (figure 5*c*). Furthermore, in order to analyse the element distribution of Ni-decorated h-BN powders, the EDS is implemented as presented in figure 5*d*$_0$–*d*$_4$. The EDS spectrum shows a strong Ni peak corresponding to the flake h-BN powders, and the element content of Ni and P are 13.69 at.% and 1.41 at.%, respectively. From figure 5*d*$_1$–*d*$_4$, it can be seen that the Ni and P elements are distributed independently on the surface or between layers of h-BN powders. This distribution serving as the dispersed Ni particles forms a Ni-decorated structure.

TEM and HRTEM analyses were carried out to get more detailed information about morphology and crystallinity of Ni-decorated h-BN powders. As shown in figure 6*a*, there are a number of nano-sized dark particles on the surface of laminar material through TEM images. Figure 6*b* is the HRTEM image of the laminar h-BN powder. The Fourier transform is obtained in the area of red square, as is presented in figure 6*b'*, the lattice fringes are clearly visible with a spacing of 0.33 nm, which is in good agreement with the spacing of the (002) plane of the crystal h-BN. The inset of figure 6*b* distinctly depicts the selected area electron diffraction (SAED) pattern of the red region; those diffraction rings are, respectively, corresponding to the crystal planes (011), (112), (006), (202) and (026). The high-index crystal faces are observed mainly owing to the relatively thin surface and the poor crystallinity of h-BN powders, but it is enough to prove that the sheet materials are h-BN powders. In order to verify the nano-sized dark little grains as Ni globules, the HRTEM image is acquired by figure 6*a*, as shown in figure 6*c*. Accordingly, the lattice fringes of dark little particles in red square are obtained by inverse Fourier transform (figure 3*b'*); it can be examined that the value of spacing is 0.203 nm. This parameter
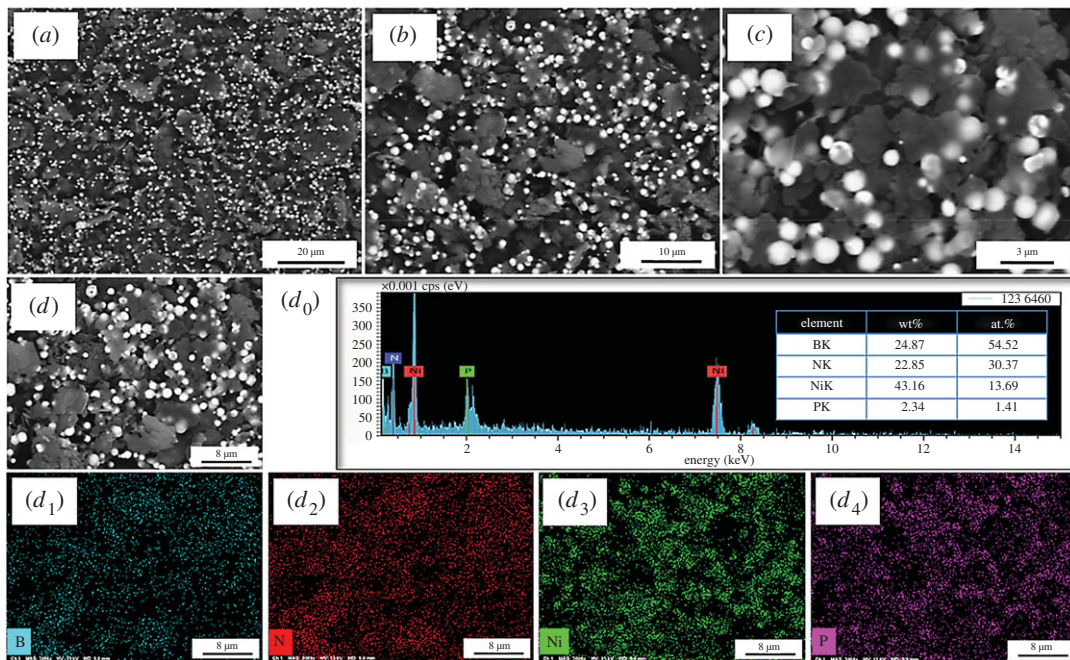
Figure 5. SEM images (a–d), EDS spectrum and mapping (d_0–d_4) of Ni-decorated h-BN powders fabricated with 30 g l^{-1} ChCl-EG as additive.
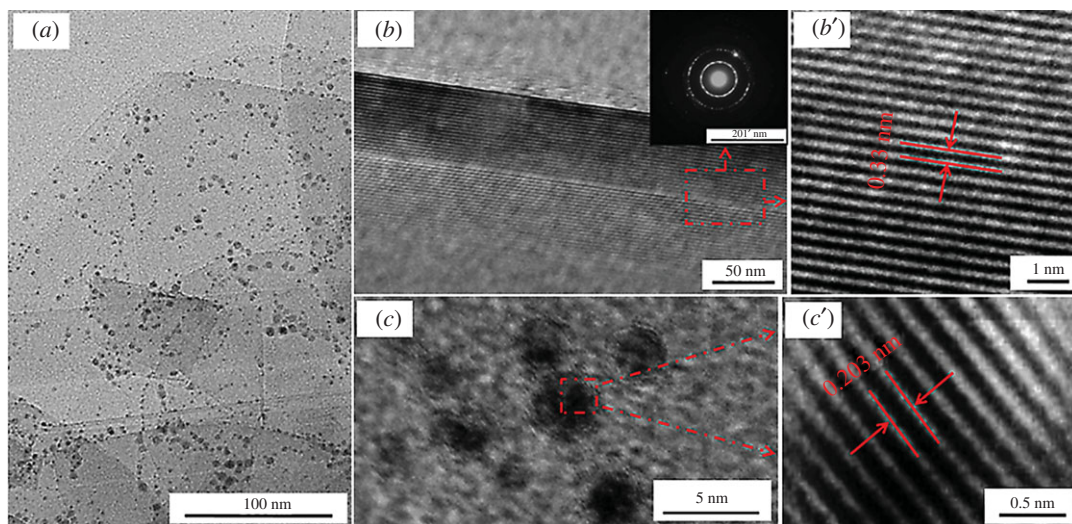

Figure 6. (a) TEM images of Ni-decorated h-BN powders with 30 g l^{-1} ChCl-EG as additive, (b,b') HRTEM images and FFT analysis of h-BN powders (inset: corresponding SAED patterns), (c,c') HRTEM images and FFT analysis of Ni grains on h-BN surface.

is consistent with the crystal plane (111) of Ni element, so the nano-sized dark particles are Ni globules, which cannot be observed with SEM due to the tiny size.

3.3. Effects of electroless plating times on Ni-decorated h-BN powders

To better analyse the deposition phenomena about Ni particles on the surface of h-BN powders, the fabrication of Ni-decorated h-BN powders is carried out without and with 30 g l^{-1} ChCl-EG as additive with one (figures 4 and 5), three (figure 7), five (figure 8) times of electroless deposition. When the Ni-decorated h-BN powders are obtained without ChCl-EG via the electroless plating one time, as shown in figure 4, little Ni particles are deposited on h-BN surface. It can be seen that a part of Ni clusters
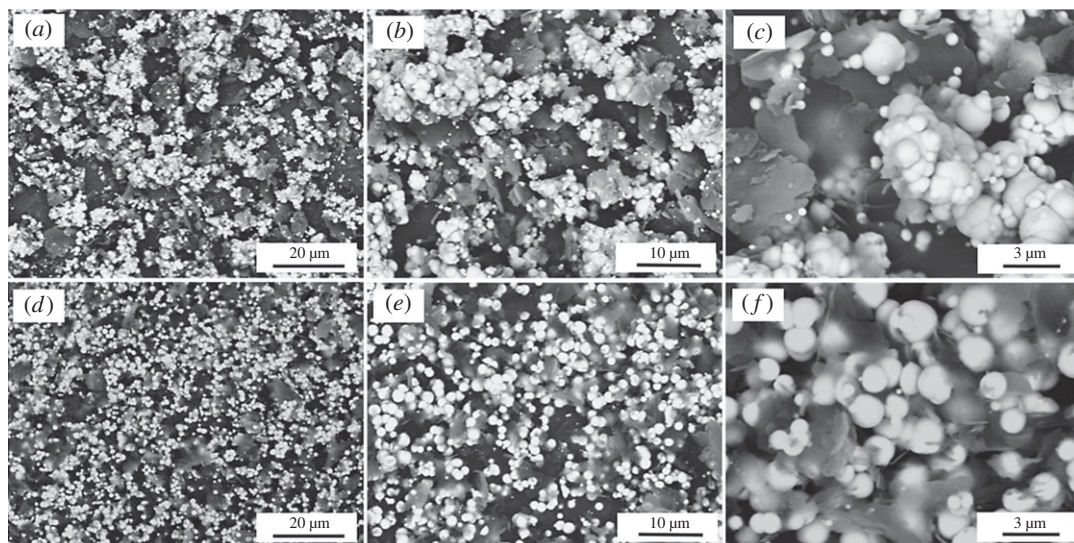
Figure 7. SEM micrographs of Ni-decorated h-BN powders with electroless plating three times: (*a–c*) without 30 g l^{-1} ChCl-EG and (*d–f*) with 30 g l^{-1} ChCl-EG as additive.

(figure 4*a* and *a₃*). However, when the Ni-decorated h-BN powders are fabricated with 30 g l^{-1} ChCl-EG via the electroless plating one time, as presented in figure 5, the distribution of Ni particles was in independently and dispersed state on h-BN powders. Moreover, those Ni particles are globular with a mean size of about 10–1000 µm (from figure 5*b–d* and *d₃*).

When the reaction times are extended to three times without ChCl-EG, as shown in figure 7*a–c*, many Ni clusters are deposited on h-BN surface and most h-BN are exposed. It indicates that most Ni particles are agglomerated without ChCl-EG as additive in the electroless bath and on the h-BN surface. While the Ni particles are uniformly and dispersedly deposited on h-BN surface with ChCl-EG as additive via plating three times, as shown in figure 7*d–f*. Thus, it is indicated that ChCl-EG as additive can effectively hinder the agglomeration of Ni particles on h-BN surface. However, it can be also seen that a small part of h-BN surface is not deposited by Ni particles (figure 7*f*).

Then, the reaction times are increased to five times in figure 8. As presented in figure 8*a–c*, it can be seen that more Ni clusters are deposited on h-BN surface and those clusters become much bigger. Besides, there is also much exposed h-BN surface. The deposition phenomenon is analogous to figure 7*a–c*. The EDS spectrum shows the element content of Ni and P are 27.90 at.% and 1.16 at.%, respectively. It indicates that more and more Ni particles are deposited on h-BN surface. Besides, it is obvious that the deposited Ni particles are in stacked state from figure 8*c₀* and *c₄*. As reaction times extended to five times with ChCl-EG as additive, as shown in figure 8*d–f*, the Ni particles are dispersedly and uniformly deposited on the surface of h-BN, compared with figure 7*a–c*. The EDS analysis indicates that the element content of Ni and P are 48.76 at.% and 6.20 at.%, respectively. The distribution of Ni particles is also dispersive, as shown in figure 8*f₀–f₅*. It demonstrates ChCl-EG as additive is beneficial to deposit Ni particles on h-BN surface. The phenomenon is consistent with figure 2*a*. Besides, Ni particles are compactly deposited on the surface of h-BN powders from figure 8*d–f₀*.

The XRD patterns of Ni-decorated h-BN powders fabricated without and with ChCl-EG as additive via the electroless plating one, three, five times are illustrated in figure 9. From figure 9*a*, it can be seen that the peak of metallic Ni is much stronger and broader at $2\theta = 44.50°$ when the reaction times are extended from plating three times to five times. The JCPDS cards of Ni and P elements are consistent with the mentioned contents in §3.1. Remarkably, the main peaks of h-BN are distinct and sharp at $2\theta = 26.74°$, being analogous to the figure 2*b*, while the other peaks of h-BN can be weakened or disappear owing to the increasing content of metallic Ni, which is in agreement with the SEM micrographs without ChCl-EG. The Ni-decorated h-BN powders are fabricated with ChCl-EG as additive, as shown in figure 9*b*. With the increase of plating times, the chance of Ni element and h-BN powders peak is analogous to figure 9*b*. It indicates that more Ni particles are deposited with the increased plating times, which is consistent with the textual SEM micrographs. From figure 9, it can be demonstrated that more and more Ni particles are deposited from sulfate solution. Therefore, the Ni-decorated h-BN structure can
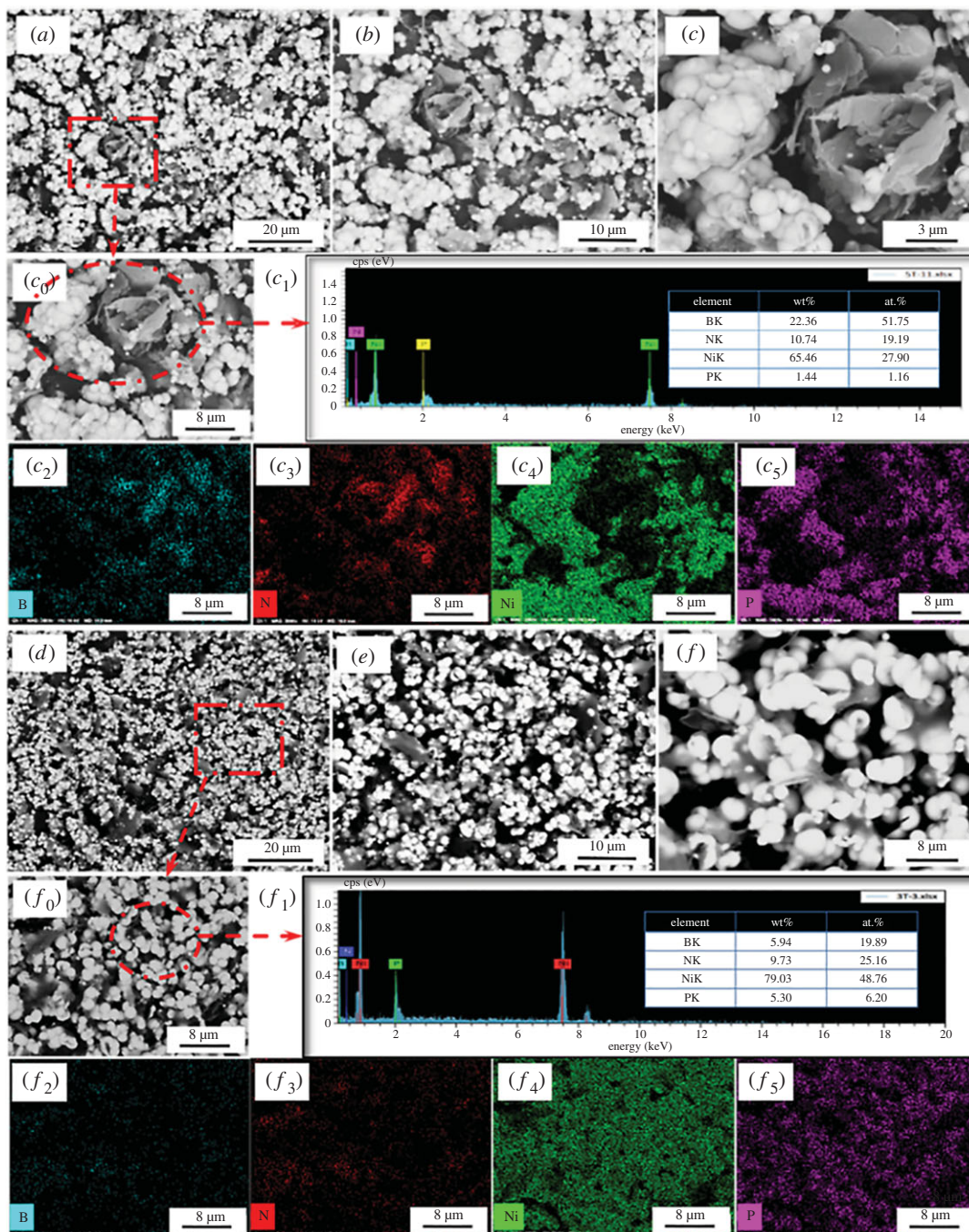
Figure 8. SEM micrographs and EDS analysis of Ni-decorated h-BN powders: (a–c_0) SEM micrographs and (c_1–c_5) EDS analysis of plating five times without ChCl-EG, (d–f_0) SEM micrographs and (f_1–f_5) EDS analysis of plating five times with 30 g l^{-1} ChCl-EG as additive.

be obtained by the deposition of metallic Ni on h-BN powders with increasing electroless plating times. Accordingly, the electroless process can be explained by the following possible deposition phenomena and growth mechanism.

3.4. Deposition phenomena and growth mechanism of Ni-decorated h-BN powders

Based on the above analysis and the relevant reference [2,44], the possible deposition phenomena and growth mechanism of Ni particles on h-BN powders without and with ChCl-EG as additive are proposed respectively, as shown in figure 10. After the pretreatment process of h-BN, the surface impurities are removed to deposit Ni particles on the h-BN surface. When the cleaned h-BN powders are introduced
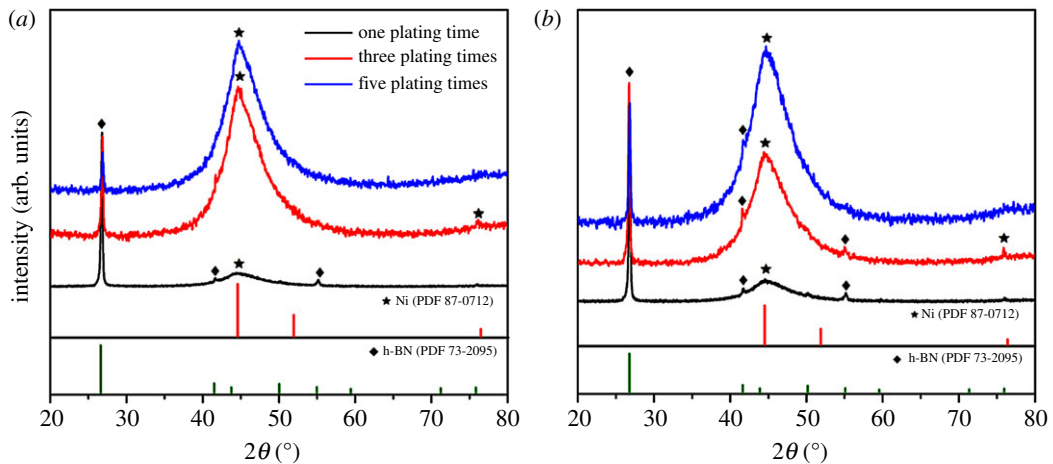
Figure 9. XRD pattern of Ni-decorated h-BN powders via the electroless plating one, three, five times: (*a*) without ChCl-EG, (*b*) with 30 g l^{-1} ChCl-EG as additive.
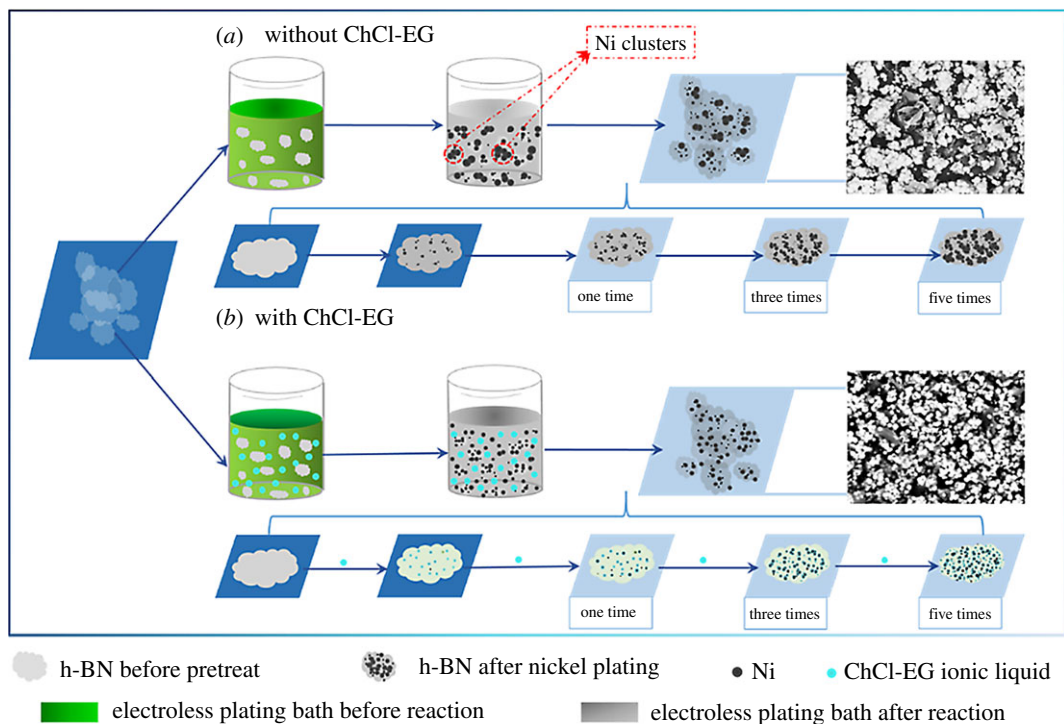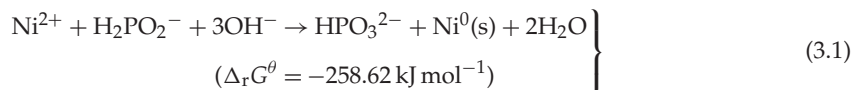

Figure 10. Electroless deposition phenomena of Ni-decorated h-BN powders: (*a*) without ChCl-EG and (*b*) with 30 g l^{-1} ChCl-EG ionic liquid as additive.
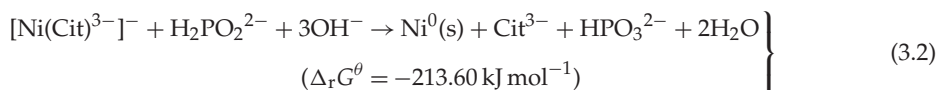
into the electroless plating solution without ChCl-EG, the Ni^{2+} and P^+ are reduced respectively into Ni and P elements by hypophosphite with the condition of temperature and stirring [33,44]. Meanwhile, the colour of the solution is turned from green to light green with little grey and a great deal of hydrogen bubbles appear together, indicating the deposition of Ni metallic with P element from the solution, as shown in equations (3.1) and (3.2). The standard free energy is the negative value, so the reaction of reducing Ni^{2+} is spontaneous [33,36,45]. Meanwhile, those energies of temperature and mechanical stirring speed were implemented to speed up the reaction.

The nano-sized Ni particles with high surface area and energy are generated in the electroless bath and on the h-BN surface, as presented in figure 10*a*. Besides, the Ni particles are easy to being the cluster on the h-BN surface powders and in the electroless solution. It is a result that the Ni particles are more

inclined to form a nucleus and grow on the original nucleation point, which is the aggregative place of Ni particle after the electroless plating one time. With the increase of plating times, the formed Ni clusters of plating one time will lead to more agglomerated state of Ni particles on the surface of h-BN powders. Meanwhile, many independently separated Ni clusters away from the h-BN surface develop the irregular dendrites and blocks, as shown in the illustration of figure 10a.

$$\left. \begin{array}{l} Ni^{2+} + H_2PO_2^- + 3OH^- \rightarrow HPO_3^{2-} + Ni^0(s) + 2H_2O \\ (\Delta_r G^\theta = -258.62 \, kJ \, mol^{-1}) \end{array} \right\} \quad (3.1)$$

and

$$\left. \begin{array}{l} [Ni(Cit)^{3-}]^- + H_2PO_2^{2-} + 3OH^- \rightarrow Ni^0(s) + Cit^{3-} + HPO_3^{2-} + 2H_2O \\ (\Delta_r G^\theta = -213.60 \, kJ \, mol^{-1}) \end{array} \right\} \quad (3.2)$$

When ChCl-EG ionic liquid is used as additive, the electroless deposition process of Ni particles on the surface of h-BN powders is extraordinarily different, as illustrated in figure 10b. The Ni particles are easy to be dispersedly and uniformly precipitated on the surface of flake h-BN powders, owing to the nucleation point may appear on the hollow surface of h-BN powders during the process. Meanwhile, the ChCl-EG additive efficiently hinders the random nucleation and agglomeration of Ni grains. This is mainly because some regions result in the adsorption of ChCl-EG, so the distribution of Ni particles was relatively homogeneous via the electroless plating one time (figure 10b).

Most regions of h-BN surface are covered by Ni particles with the increase of plating times, which is mainly because Ni particles are easy to nucleate and grow on the formed Ni globules of the first electroless plating, as is shown in the illustration of figure 10a. When the reaction was beginning, some tiny Ni particles deposited randomly on the surface of h-BN powders. As the reaction proceeding, a part of Ni particles is gradually growing on the original site, and those particles are bigger and bigger. Besides, some new Ni particles nucleation points can be found on h-BN surface. The Ni-decorated h-BN powders are fabricated with ChCl-EG by plating one time, but the Ni particles are dispersedly deposited with less number. In order to deposit uniformly Ni particles on the surface of h-BN, the electroless plating times were extended to three times and five times. Correspondingly, the Ni particles are compactly and uniformly deposited on the surface of h-BN powders, as can be presented from figure 8f and the illustration of figure 10b. Hence, some dispersedly and compactly Ni-decorated h-BN powders can be obtained via the electroless plating with ChCl-EG ionic liquid as additive.

4. Conclusion

(1) The Ni particles are more intended to be dispersedly deposited on h-BN surface from 0 to 30 g l^{-1} ChCl-EG ionic liquid. Then, when the ChCl-EG additive is increased from 30 to 90 g l^{-1}, the distribution of Ni particles on h-BN surface comes gradually into being the aggregated state and have the tiny size. Therefore, the addition of 30 g l^{-1} ChCl-EG ionic liquid is optimum to obtain the independently and uniformly Ni particles on the h-BN surface by electroless deposition.
(2) The deposited Ni particles from sulfate solution can be distributed on the h-BN powders by electroless deposition with 30 g l^{-1} ChCl-EG ionic liquid as additive. The Ni particles on h-BN surface are spheroidal with a mean size 10–1000 nm.
(3) The deposition phenomena of Ni-decorated h-BN powders are studied with the increase of the electroless plating times based on the changes in morphology. Ni clusters are more and more without ChCl-EG. Conversely, Ni particles can be dispersedly and uniformly on h-BN surface with ChCl-EG as additive.
(4) The deposition phenomena and growth mechanism of Ni-decorated h-BN powders are put forward. The mechanism emphasizes that 30 g l^{-1} ChCl-EG as additive is more prone to form the dispersed and uniform Ni particles on the surface of h-BN powders to gain the Ni-decorated h-BN powders without Ni clusters.

References

1. Keong KG, Sha W. 2002 Crystallisation and phase transformation behaviour of electroless nickel-phosphorus deposits and their engineering properties. *Surf. Eng.* **18**, 329–343. (doi:10.1179/026708402225010010)

2. Ru JJ, Jia Y, Jiang YH, Feng J, R. Zhou, Hua YX. 2017 Modification of ZTA particles with Ni coating by electroless deposition. *Surf. Eng.* **33**, 353–361. (doi:10.1080/02670844.2016.1248119)

3. Li XQ, Gao YM, Yang QX. 2017 Sliding tribological performance of B_4C-hBN composite ceramics against AISI321 steel under distilled water condition. *Ceram. Int.* **43**, 14 932–14 937. (doi:10.1016/j.ceramint.2017.08.010)

4. Brenner A, Riddell GE. 1946 Nickel plating on steel by chemical reduction. *J. Res. Natl Bur. Stand.* **37**, 31–34. (doi:10.6028/jres.037.019)

5. Bello KA, Maleque MA, Ahmad Z. 2015 Synthesis and characterization of Ni–P coated hexagonal boron nitride by electroless nickel deposition. *Surf. Eng. Appl. Electrochem.* **51**, 523–529. (doi:10.3103/S1068375515060058)

6. Li XQ *et al.* 2018 Influences of hBN content and test mode on dry sliding tribological characteristics of B_4C-hBN ceramics against bearing steel. *Ceram. Int.* **44**, 6443–6450. (doi:10.1016/j.ceramint.2018.01.039)

7. Kumar MA, Agarwala RC, Agarwala V. 2008 Synthesis and characterization of electroless Ni-P coated graphite particles. *Bull. Mater. Sci.* **31**, 819–824. (doi:10.1007/s12034-008-0130-1)

8. Gu JW, Lv ZY, Wu YL, Guo YQ, Tian LD, Qiu H, Li WZ, Zhang QY. 2017 Dielectric thermally conductive boron nitride/polyimide composites with outstanding thermal stabilities via *in-situ* polymerization-electrospinning-hot press method. *Compos. Part A Appl. Sci. Manuf.* **94**, 209–216. (doi:10.1016/j.compositesa.2016.12.014)

9. Li XQ, Gao YM, Wei SZ, Yang QX. 2017 Tribological behaviors of B_4C-hBN ceramic composites used as pins or discs coupled with B_4C ceramic under dry sliding condition. *Ceram. Int.* **43**, 1578–1583. (doi:10.1016/j.ceramint.2016.10.136)

10. Zou TZ, Tu JP, Zhang SC, Chen LM, Wang Q, Zhang LL, He DN. 2006 Friction and wear properties of electroless Ni-P-(IF-MoS_2) composite coatings in humid air and vacuum. *Mater. Sci. Eng. A* **426**, 162–168. (doi:10.1016/j.msea.2006.03.068)

11. Sudagar J, Lian J, Sha W. 2013 Electroless nickel, alloy, composite and nano coatings — a critical review. *J. Alloys Compd.* **571**, 183–204. (doi:10.1016/j.jallcom.2013.03.107)

12. Balaraju JN, Narayanan TSN, Seshadri SK. 2003 Electroless Ni–P composite coatings. *J. Appl. Electrochem.* **33**, 807–816. (doi:10.1023/A:1025572410205)

13. Kretz F, Gácsi Z, Kovács J, Pieczonka T. 2004 The electroless deposition of nickel on SiC particles for aluminum matrix composites. *Surf. Coat. Technol.* **180**, 575–579. (doi:10.1016/j.surfcoat.2003.10.150)

14. Lin CJ, Chen KC, He JL. 2006 The cavitation erosion behavior of electroless Ni–P–SiC composite coating. *Wear* **261**, 1390–1396. (doi:10.1016/j.wear.2006.03.054)

15. Gu JW, Guo YQ, Yang XT, Liang CB, Geng WC, Tang L, Li N, Zhang QY. 2017 Synergistic improvement of thermal conductivities of polyphenylene sulfide composites filled with boron nitride hybrid fillers. *Compos. Part A Appl. Sci. Manuf.* **95**, 267–273. (doi:10.1016/j.compositesa.2017.01.019)

16. Afroukhteh S, Dehghanian C, Emamy M, Afroukhteh S, Dehghanian C, Emamy M. 2012 Preparation of the Ni–P composite coating co-deposited by nano TiC particles and evaluation of its corrosion property. *Appl. Surf. Sci.* **258**, 2597–2601. (doi:10.1016/j.apsusc.2011.10.101)

17. Jafari M, Enayati MH, Salehi M, Nahvi SM, Park CG. 2014 Microstructural evolution of nanosized tungsten carbide during heatup stage of sintering of electroless nickel-coated nanostructured WC–Co powder. *Ceram. Int.* **40**, 11 031–11 039. (doi:10.1016/j.ceramint.2014.03.118)

18. Luo L, Yu J, Luo J, Li J. 2010 Preparation and characterization of Ni-coated CrC powder by room temperature ultrasonic-assisted electroless plating. *Ceram. Int.* **36**, 1989–1992. (doi:10.1016/j.ceramint.2010.03.003)

19. Chuankrerkkul N, Boonyongmaneerat Y, Saengkiettiyut K, Rattanawaleedirojn P, Saenapitak S. 2013 Injection moulding of tungsten carbide-nickel powders prepared by electroless deposition. *Key Eng. Mater.* **545**, 148–152. (doi:10.4028/www.scientific.net/KEM.545.148)

20. Gu JW, Xu S, Zhuang Q, Tang YS, Kong J. 2017 Hyperbranched polyborosilazane and boron nitride modified cyanate ester composite with low dielectric loss and desirable thermal conductivity. *IEEE Trans. Dielect. Electr. Insul.* **24**, 784–790. (doi:10.1109/TDEI.2017.006299)

21. Mafi IR, Dehghanian C. 2011 Comparison of the coating properties and corrosion rates in electroless Ni–P/PTFE composites prepared by different types of surfactants. *Appl. Surf. Sci.* **257**, 8653–8658. (doi:10.1016/j.apsusc.2011.05.043)

22. Wu YT, Zhong C, He MF, Liu L, Hu WB. 2011 Antifriction and wear characteristics of electrolessly-deposited Ni–P with PTFE composites. *Trib. Lett.* **42**, 161–168. (doi:10.1007/s11249-011-9759-9)

23. Liew K W, Chia SY, Kok CK, Low KO. 2013 Evaluation on tribological design coatings of Al_2O_3, Ni–P–PTFE and MoS_2 on aluminium alloy 7075 under oil lubrication. *Mater. Des.* **48**, 77–84. (doi:10.1016/j.matdes.2012.08.010)

24. Wei XF, Wang RC, Feng Y, Zhu XW. 2001 Influence of hexagonal boron nitride (hBN) powders coated with Ni on properties of Ni-Cr/hBN self-lubricating composite. *Mater. Sci. Eng. Pow. Metall.* **19**, 86–92.

25. Kong XL, Liu YB, Lu Y, Huo FX. 2001 P/M metal-matrix high-temperature solid self-lubricating materials. *Pow. Metal. Technol.* **19**, 86–92.

26. Kimura Y, Wakabayashi T, Okada K, Wadac T, Nishikawad H. 1999 Boron nitride as a lubricant additive. *Wear* **232**, 199–206. (doi:10.1016/S0043-1648(99)00146-5)

27. Palaniappa M, Babu GV, Balasubramanian K. 2007 Electroless nickel–phosphorus plating on graphite powder. *Mater. Sci. Eng. A* **471**, 165–168. (doi:10.1016/j.msea.2007.03.004)

28. Chen WX, Tu JP, Gan HY, Xu ZD, Wang QG, Lee JY, Liu ZL, Zhang XB. 2002 Electroless preparation and tribological properties of Ni-P-Carbon nanotube composite coatings under lubricated condition. *Surf. Coat. Technol.* **160**, 68–73. (doi:10.1016/S0257-8972(02)00408-5)

29. Alishahi M, Hosseini SM, Monirvaghefi SM, Saatchi A. 2013 Synthesis and passivation behavior of electroless Ni-P-CNT composite coating. *Mater. Corros.* **64**, 212–217. (doi:10.1002/maco.201106136)

30. Du LZ, Zhang WG, Liu W, Zhang JM. 2010 Preparation and characterization of plasma sprayed Ni_3Al–hBN composite coating. *Surf. Coat. Technol.* **205**, 2419–2424. (doi:10.1016/j.surfcoat.2010.09.036)

31. Gu JW, Liang CB, Dang J, Dong WC, Zhang QY. 2016 Ideal dielectric thermally conductive bismaleimide nanocomposites filled with polyhedral oligomeric silsesquioxane functionalized nanosized boron nitride. *Rsc Adv.* **6**, 35 809–35 814. (doi:10.1039/c6ra04513h)

32. Zhang ST, Zhou JS, Guo BG, Zhou HD, Pu YP, Chen JM. 2009 Friction and wear behavior of laser cladding NiAl/hBN self-lubricating composite coating. In *Advanced tribology* (eds J Luo, Y Meng, T Shao, Q Zhao), p. 442. Berlin, Germany: Springer.

33. Gu JW, Zhang GC, Dong SL, Zhang QY, Kong J. 2007 Study on preparation and fire-retardant mechanism analysis of intumescent flame-retardant coatings. *Surf. Coat. Technol.* **201**, 7835–7841. (doi:10.1016/j.surfcoat.2007.03.020)

34. Li F, Wang X, Zhang M, Zhang D. 2006 Optimization of process parameters of nickel coated on the boron nitride ceramic particles by chemical plating. *J. Chin. Ceram. Soc.* **34**, 1112.

35. Zhao J, Zhou J, Guo C, Yu Y, Zhou H, Chen J. 2010 Preparation of nickel-coated hexagonal BN particles by hydrothermal hydrogen reduction. *Chin. Pow. Sci. Technol.* **16**, 8–13.

36. Gu JW, Meng XD, Tang YS, Li Y, Zhuang Q, Kong J. 2016 Hexagonal boron nitride/polymethyl-vinyl siloxane rubber dielectric thermally conductive composites with ideal thermal stabilities. *Compos. A Appl. Sci. Manuf.* **92**, 27–32. (doi:10.1016/j.compositesa.2016.11.002)

37. Mallory GO, Hajdu JB. 1990 *Electroless plating: fundamentals and applications*. Norwich, NY: William Andrew.

38. Holbrey JD, Rogers RD. 2002 Green industrial applications of ionic liquids: technology review. *ACS*

Pub. **34**, 446–458. (doi:10.1021/bk-2002-0818. ch034)

39. Kondo Y, Sasaki T, Sasaki S. 2013 Tribological properties of ionic liquids. *Int. Jpn*. **5**, 127–141. (doi:10.5772/52595)

40. Somers AE, Howlett PC, Macfarlane DR, Forsyth M. 2013 A review of ionic liquid lubricants. *Lubricants* **1**, 3–21. (doi:10.3390/lubricants1010003)

41. Welton T. 2004 Ionic liquids in catalysis. *Coord. Chem. Rev.* **248**, 2459–2477. (doi:10.1016/j.ccr. 2004.04.015)

42. Xiao XH, Zhao L, Liu X, Jiang SX. 2004 Ionic liquids as additives in high performance liquid chromatography: analysis of amines and the interaction mechanism of ionic liquids. *Ana. Chimica Acta* **519**, 207–211. (doi:10.1016/j.aca.2004.06.038)

43. Zhang QB, Wang R, Chen KH, Hua YX. 2014 Electrolysis of solid copper oxide to copper in choline chloride-EG eutectic melt. *Electrochim. Acta* **121**, 78–82. (doi:10.1016/j.electacta.2013.12.114)

44. Uysal M, Karslioğlu R, Alp A, Arbulut H. 2013 The preparation of core−shell Al_2O_3/Ni composite

powders by electroless plating. *Ceram. Int.* **39**, 5485–5493. (doi:10.1016/j.ceramint.2012.12.060)

45. Li XQ, Gao YM, Wei SZ, Zhong ZC. 2017 Dry sliding tribological properties of self-mated couples of B4C-hBN ceramic composites. *Ceram. Int.* **43**, 162–166. (doi:10.1016/j.ceramint.2016.09.128)

46. Yang Q, Ru J, Song P, Hu M, Feng J. 2018 Data from: Fabrication and characterization of Ni-decorated h-BN powders with ChCl-EG ionic liquid as addition by electroless deposition. Dryad Digital Repository. (doi:10.5061/dryad.f2579)